Electric Power Systems Research 205 (2022) 107772

Contents lists available at ScienceDirect

Electric Power Systems Research

journal homepage: www.elsevier.com/locate/epsr

Online estimation of thévenin equivalent using discrete fourier transform

Abdelrahman Sobhy [a], Mohammed A. Saeed [b], Abdelfattah A. Eladl [b,*], Sobhy M. Abdelkader [a,b]

[a] Electrical Power Engineering Department, Egypt-Japan University for Science and Technology (E-JUST), New Borg El-Arab, Alexandria, Egypt
[b] Electrical Engineering Department, Faculty of Engineering, Mansoura University, Egypt

ARTICLE INFO

Keywords:
Discrete fourier transform
PMU
Power system equivalents
Thévenin equivalent

ABSTRACT

This paper presents a method for the determination of the Thévenin equivalent (TE) parameters of a power system using local phasor measurement unit (PMU) measurements. The proposed method is based on an innovative use of Discrete Fourier Transform (DFT), where the DFT coefficients are calculated for the measured voltage and current phasors, which are used to determine the TE parameters. The method presented exploits the characteristics of DFT to develop a new simple and efficient method for TE determination. The calculated DFT is also utilized to detect the presence of measurement errors and to get the best estimate of TE parameters in such conditions and also enable identification of the erroneous measurement. The proposed method is illustrated using a simple system and tested with the data of standard test systems, which all verified the accuracy of the proposed method.

1. Introduction

The ability to represent a system by a simple equivalent, while keeping the local performance indicators, makes Thévenin Equivalent (TE) one of the mostly used tools over more than a century. Even though the power system has witnessed drastic changes, there were always needs and applications for TE. These include, but are not limited to, fault analysis [1], a linear indicator for voltage collapse [2], voltage stability analysis [3–7], adaptive design of a protection scheme for the power system [8], prediction of rotor angle stability [9], identification of photovoltaic array faults using TE resistance [10], estimating the maximum emergency power capacity of line-commutated-converter in HVDC system [11], and calculating indicator for cyber-attacks on phasor measurement unit (PMU) data using the TE parameters of the multi-port equivalent circuit [12].

TE parameters calculated from two endpoints of interest in any linear time-invariant network satisfy the following equation:

$$E_{th} = I_{sc}\ Z_{th} \tag{1}$$

where E_{th} is the TE open-circuit voltage, Z_{th} is the TE impedance, and I_{sc} is the short circuit current. This may assume that direct measurement of open-circuit voltage and short circuit current is an easy way to calculate these quantities, but this involves active circuit manipulation and is not technically allowable to make deliberate short circuits. Moreover, transients corresponding to the short circuit will not enable reliable phasor measurements. Analytical methods used to obtain the TE parameters require complete access to the network's topology and characteristics, which are not available for local access. Typically, the information accessible at the relevant terminals is limited to r.m.s or time-domain voltages/currents at one or more operating points. This is why methods for determining TE from local measurements are highly demanded, especially with the changes in power systems that give rise to different competing players who have no access rights to the full system data. Such a situation arises with the restructuring of power systems and gets more evident with the booming integration of renewable energy systems and distributed generation. The methods for TE parameters determination can be divided into two categories: noninvasive approaches and invasive approaches.

Invasive approaches intentionally disrupt the system, then evaluate the response to estimate the TE parameters [13]. These methods necessitate a significant number of measurements with a relatively large gap. The two-point technique and the extended three-point method, as well as recursive and least-squares approaches, are often used algorithms, as mentioned in [4,14–16]. Typically, a step or an impulse is applied to the local system's input voltage to observe the current response [17]. While these methods can be used to determine the TE parameters, they have the disadvantage of introducing perturbations. Adaptive Kalman filter-based approaches and extended Kalman filter-based approaches are also capable of accurately estimating TE parameters while minimizing the requirement for system perturbation.

* Corresponding author.
E-mail address: eladle7@mans.edu.eg (A.A. Eladl).

https://doi.org/10.1016/j.epsr.2022.107772
Received 14 October 2021; Received in revised form 16 December 2021; Accepted 1 January 2022
Available online 5 January 2022

Rather than that, they rely on the network's inherent disturbances for excitation [18].

Noninvasive approaches for identifying the true value of the power system impedance are mostly used to determine the voltage change at a particular network location caused by an observed current change (mainly load current) [19,20]. The power system's response to a change in recorded load current is not always the same because the current of parallel loads, the power system's impedance, or the voltage of an equivalent voltage source can change suddenly. As a result, these approaches rely on higher sample size. Although noninvasive methods do not intentionally disrupt the system, they have a big disadvantage is that measurement points must be computed at many static instances, which introduces the possibility of erroneous estimations due to voltage fluctuation, phase drift, and non-synchronized measurements [5]. The authors in [21] presented the development of a time-domain dynamic model for the purpose of online estimation of Thevenin's equivalent impedance of a network as seen from a bus. According to [22] a normal recursive least square algorithm is used to track probable parameter changes after a specified amount of time. In [23], the nodal voltage equation was employed to generate a high dimensional linear system to acquire the equivalent voltage, and the lower–upper factorization was used to obtain a speedy and accurate estimation of TE parameters.

Recently, more attention has been focused on the detection of TE based on local PMU measurement data [24]. These methods do not require network topology but require local measurement information. These algorithms are founded on the concept that TE remains constant across the sampling period [6], and the equivalent parameter is identified using repeated cross-sectional data. In [25], the comparable reduction in the power flow model was derived directly by applying the least square approach to the boundary bus measured value to determine multiport TE circuit parameters. The authors in [26] proposed a fast-tracking Thévenin parameter technique for filtering out oscillations without considerably delaying the recognition process. However, difficulties like line tripping, shunt capacitor switches, and generators exceeding their reactive power output limits will occur in practical systems [7]. These issues contribute to the method's abovementioned inaccuracies. As a result, the issue of parameter drift because of time-varying operating conditions becomes critical [27]. To improve these methods, the literature [28] advocated calculating the impedance of the online Thévenin at the generator terminal using the frequency change rate available at the PMU's output to compensate for phase drift's detrimental impacts. Using Tellegen's theorem and two measurements in [29], the expression for equivalent impedance was derived. Then, based on technique [30], the Thévenin index was derived.

Additionally, the measured value of PMU data captured may differ from the real value due to external interference or system malfunction [31]. To address this issue, some scholars have attempted to alleviate problems caused by erroneous data using state estimate approaches [31–34]. The study in [32] provided an optimal approach for estimating the parameters of the Thévenin model that did not need solving a system of nonlinear equations with measurement and quantization noise. In [33], a graphical technique for obtaining TE was devised based on the representation and manipulation of observed voltage phasors in the complex voltage plane. Authors in [35] suggested an expanded Kalman filtering method based on the equivalency constraint, which utilized a statistical projection algorithm to increase the robustness of leverage measurements. The work in [4] used a robust recursive least squares approach to detect and deal with measurement outliers and missing data. A regular term was incorporated into the robust least-squares estimate to actualize the model parameters' previous conjecture, and the anti-interference capacity of measurement noise and gross error was improved in [36]. Authors in [37] proposed an extended multivariate Huber loss function for parameter estimation in a linear model with non-gaussian noise.

The procedures outlined above have significantly decreased the impact of erroneous measurements and noise on some PMU measurement results. However, their performances are insufficient to address the issue of algorithm divergence induced by the erroneous conditioned matrix inverse, they lack robustness and adaptive tracking when the system changes. Using Schmidt's orthogonalization transformation, authors in [38] proposed a method for getting exact solutions to the Thevenin equivalent parameters equations with erroneous initial conditions. In [39], a methodology for estimating dynamic states was suggested that integrated a novel regularization-based method with a Markov model representation to increase estimation accuracy compared to traditional methods based on static load pseudo measurements. In [40], adaptive adjustment of the forgetting factor increased the tracking performance of the resilient recursive least square algorithm, which was then utilized to estimate electromechanical modes in power systems. The study in [41] described how to include a pseudo-random binary sequence into the control loop of a grid-connected inverter to estimate power system impedance under unbalanced grid conditions. In the case of connecting distributed generators to the grid using three-phase inverters, impedance calculation can be performed using the variations in active and reactive power injected by these inverters [42].

Table 1 summarizes a general comparison between the previous literature techniques to estimate TE parameters.

The wide range of TE applications that covers most of the power system aspects makes it a kind of general-purpose tool. Therefore, there will be always a need for methods of finding reliable TE parameters. This paper presents a new method for the online determination of TE using PMU measurements and Discrete Fourier Transform (DFT). The proposed method exploits the interesting features of DFT of having self-check for the accuracy of the determined TE parameters and the ability to identify erroneous measurements with a proper manipulation of DFT coefficients. In a previous paper [27], the authors presented a method for online tracking of TE parameters with the number of measurements during the calculation step is limited to three and the use of five measurements was recommended in [31]. The new method proposed in this paper can use a data window with any required length. It is simple and determines TE parameters in an explainable manner that makes it suitable for both real system applications as well as educational purposes.

The rest of the paper is organized by introducing the proposed method in section II, just following this introduction. A detailed

Table 1
A general comparison of TE estimation techniques.

Item	Non-Invasive Techniques	Invasive Techniques
Theory	– It is based on direct measurements and there is no signal injection into the power system	– It involves injection of uncommon voltage or current harmonic at a specific frequency into the power system
Available Technology	– PMUs	– Power Converters
Implementation	– Online monitoring	– Done periodically
Advantages	– Statistical evaluation of a larger – number of samples – Implementation is straightforward	– Parameters are obtained ad-hoc, and the precision of the result is controlled. – Phase angle is not required in the calculation assuming that the grid's impedance-frequency curve is linear
Challenges	– Grid's impedance changes may be negligible as they are much slower than the rate of sampling of a PMU – Grid's frequency is not constant – Noise and error in measurements – The load side must change	– Grid's impedance is not constant – Limitations of available technology such as power electronics devices – Distortion of grid – Interference between devices

illustrative example is presented in section III using a simple two-node system explaining the calculation steps as well as detection and exclusion of bad data. Also, presents the results of applications to the IEEE 30 bus test system and to real PMU measurements. Section IV presents the conclusion followed by the list of references.

2. The proposed method

This section presents the theoretical foundations of the proposed method along with simple illustrative examples. Practical considerations of application to real-time measurements of a real power system are also discussed. Provisions for dealing with measurements having erroneous data are also presented along with example calculations.

2.1. Theoretical backgrounds and practical considerations

The proposed method utilizes the features of DFT for the determination of the Thévenin equivalent parameters using PMU measurements. It is to be made clear that the standard FT transforms a signal from the time domain to the frequency domain. However, the work of this paper has no interest in transforming any domain to another. The main interest of this work in DFT is just its mathematical process as it has interesting features that can help in determining the Thévenin equivalent parameters. In addition, DFT can enable dealing with erroneous data and determine the best estimate of the Thévenin equivalent. The general formula of DFT coefficients for N-measured samples of a variable x is given by:

$$X_k = \sum_{n=1}^{N} x_n \, \alpha^{(n-1)(k-1)}, 1 \le k \le N \tag{2}$$

where X_k is the k^{th} coefficient of DFT, x_n is the n^{th} measured phasor of voltage or current, and $\alpha = e^{\frac{-j2\pi}{N}}$. It is useful to recall the important characteristic of α that its powers from 0 to $N-1$ sum up to zero for all values of N. That is:

$$\sum_{m=0}^{N-1} \alpha^m = 0 \tag{3}$$

Although DFT can handle any number of measurements at a time, it would be better not to use a number of measurements that span a long time to avoid system side changes. Theoretically, only two voltage/current measurements, with the system side unchanged, will be sufficient for determining the Thévenin equivalent. However, due to the small changes in the system side, redundant measurements are used to account for the system side changes as well as measurement errors. In this work, five measurements are used to illustrate the proposed method and it was reported in [31] that five measurements are sufficient to determine a good Thévenin equivalent and ensure updating this equivalent in a short time interval, 2 msec. in a 50 Hz system.

The concept of Thévenin equivalent determination using local measurements is illustrated in Fig. 1, where the system side is assumed unchanged over the calculation period while the load side is changing. The load side may be a load, a local generation facility, or any small system connected to the main system at the terminals ***a*** and ***b***. Actually, both sides are changing, but the changes in the load side are much faster

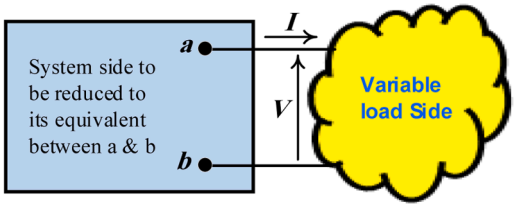

Fig. 1. System equivalence.

than that of the grid side. Voltage and current phasors are available from PMU measurements, usually one (voltage, current) pair per one power frequency cycle.

The n^{th} measured voltage/current pair (V_n, I_n) at the node of interest is related to the Thévenin equivalent parameters of the system as given by (3).

$$V_n = E_{th} - I_n \, Z_{th} \tag{4}$$

where E_{th} is the equivalent voltage source of the reduced system, Z_{th} is the equivalent impedance of the reduced system, and n indicates the order of measured samples. DFT is applied to the measurements. As mentioned above, measured voltage and current phasors, rather than instantaneous time samples will be used. So, the DFT is applied to N pairs of measured voltage and current phasors.

$$\mathbf{V_k} = \sum_{n=1}^{N} V_n \, \alpha^{(n-1)(k-1)}, \; 1 \le k \le N \tag{5}$$

$$\mathbf{I_k} = \sum_{n=1}^{N} I_n \, \alpha^{(n-1)(k-1)}, \; 1 \le k \le N \tag{6}$$

With the assumption that the system side has not changed during the time of the N measurements; all the measured (V, I) pairs will satisfy Eq. (4). Substituting for V_n in (5) by its value defined by (4), we get

$$\mathbf{V_k} = \sum_{n=1}^{N} (E_{th} - Z_{th} I_n) \, \alpha^{(n-1)(k-1)}, \; 1 \le k \le N \tag{7}$$

Hence, for $k = 1$,

$$\mathbf{V}_1 = \sum_{n=1}^{N} (E_{th} - Z_{th} I_n) = N. \, E_{th} - \sum_{n=1}^{N} Z_{th} I_n$$

And finally, at $k = 1$, we have

$$\mathbf{V}_1 = N \, E_{th} - \mathbf{I}_1 Z_{th} \tag{8}$$

For $k = 2$

$$\mathbf{V}_2 = \sum_{n=1}^{N} E_{th} \, \alpha^{(n-1)} - Z_{th} \sum_{n=1}^{N} I_n \, \alpha^{(n-1)} = E_{th} \sum_{m=0}^{N-1} \alpha^m - Z_{th} \sum_{n=1}^{N} I_n \, \alpha^{(n-1)}$$

It follows from (3) that the first term on the right-hand side of the above equation equals zero and hence,

$$\mathbf{V}_2 = -\mathbf{I}_2 \, Z_{th} \tag{9}$$

It can be proved that (9) is valid for all values of $k > 1$. Thus, the Thévenin impedance can be calculated from the DFT coefficients as follows:

$$Z_{th} = \frac{-\mathbf{V_k}}{\mathbf{I_k}}, \; 2 \le \; k \; \le N \tag{10}$$

Having Z_{th} obtained from (10), E_{th} can be determined using (8) as:

$$E_{th} = \frac{\mathbf{V}_1 + Z_{th}\mathbf{I}_1}{N} \tag{11}$$

It is to be mentioned that (10) does not only give a value for Z_{th}, but also provides a means for testing the validity of this value. For the N measurements used, (10) provides $N - -1$ values for Z_{th}, which when are all equal indicate for perfect and error-free measurements and the accuracy of the estimated Z_{th}. However, real system measurements are not perfect. This is because the measuring instruments are not 100% accurate and allow for a tolerance depending on the quality of the device. This tolerable measurement error will be present almost all the time and will affect the estimated Z_k values, which will not be equal. The differences between Z_k values will depend on the value of the measurement error and hence a tolerance should be expected, and accepted, in the estimated Z_{th}. Accepted tolerance can be set separately to the

resistive and reactive components of Z_k. However, a tolerance, ε is set to the magnitude of Z_k.as it includes both components and it is more indicative of the closeness of the estimated values to each other.

Hence, if the Z_k values are not equal, the first thing to do is to check whether the estimated values are all within the accepted tolerance or not. To do that, the average value for Z_k is determined as follows.

$$Z_{av} = \frac{1}{N-1}\sum_{k=2}^{N}\frac{-\mathbf{V_k}}{\mathbf{I_k}} \tag{12}$$

Then, the deviation of each of the estimated Z_k values from the average is determined and compared to the allowable tolerance.

$$\Delta Z_k = |Z_k - Z_{av}|,\ k = 2,\ldots,N \tag{13}$$

If $\Delta Z_k \le \varepsilon, \forall k \in [2,N]$, then $Z_{th} = Z_{av}$, and E_{th} is calculated using (11). Should one or more of the ΔZ_k exceed the allowable tolerance, ε, indicates for the presence of bad or erroneous measurements and a procedure to account for erroneous measurements is to be initiated.

2.2. Accounting for erroneous data

In the presence of measurement errors, estimating a reliable TE by direct use of the measurements would not be possible. Measurement errors are not the only cause of troubling the TE determination. System side changes may disturb the calculation of the TE and compromise its validity. Several methods for tackling measurement errors and system side changes have been proposed. Moreover, most of the methods for TE parameters calculation require additional computation to test for measurement errors and/or the validity/accuracy of the determined TE [31].

This section presents a simple, yet effective, method for finding the best estimate of TE parameters out of imperfect measurements and/or system side conditions. These conditions manifest itself through large differences in the estimated values of Z_k. The proposed method builds on two salient characteristics of DFT. The first is that, for error-free measurements, the ratio of DFT voltage coefficient to the DFT current coefficient is equal to Z_{th}, which implies that the ratio of the sum/difference of two voltage coefficients to the sum/difference of the corresponding current coefficients will also equal to Z_{th}. The second is that the effect of error in one measurement sample is not the same on the different DFT coefficients, due to the different phase shifts applied to samples while determining the different DFT coefficients. So, there will be some DFT coefficients with much smaller errors than the others and hence having the least error in the estimated TE parameters.

Bearing in mind that in case of unequal values of Z_k for the different DFT coefficients, it is not possible to determine which one is the nearest to the unknown correct value. Therefore, a method for testing DFT coefficients, two at a time, against the condition of measurement accuracy is introduced. An error indicator is defined below, from which the coefficient of the best estimate for Z_{th} can be determined.

For perfect measurements and system conditions, (10) is valid and hence for any two DFT coefficients:

$$\frac{-\mathbf{V_i}}{\mathbf{I_i}} = \frac{-\mathbf{V_j}}{\mathbf{I_j}} = Z_{th} \tag{14}$$

It follows from proportionality rules that the difference of voltage coefficients divided by the difference of current coefficients equal to Z_{th}; this will be termed as Z_{ij}^{-}. It is also true that the sum of the voltage coefficients divided by the sum of the current coefficients equals Z_{th}; this will be termed as Z_{ij}^{+}.

$$Z_{ij}^{+} = \frac{-\mathbf{V_i} - \mathbf{V_j}}{\mathbf{I_i} + \mathbf{I_j}} \tag{15}$$

$$Z_{ij}^{-} = \frac{-\mathbf{V_i} + \mathbf{V_j}}{\mathbf{I_i} - \mathbf{I_j}} \tag{16}$$

The difference, ϵ_{ij}, between Z_{ij}^{+} and Z_{ij}^{-}, must be zero at the ideal case, or within acceptable tolerance considering the accuracy of measuring instruments. Hence, this difference is used as an indicator for the accuracy of the estimated Z_{th} by a DFT coefficient. The DFT coefficient, k, that gives the best estimate for Z_{th} is the one which has the minimum summation of ϵ_{kj}, where $j = 2,\ldots,\ N, j \ne k$. Therefore, if there are deviations greater than the allowable tolerance in Z_k values from the average, the steps of determining the best estimate of Z_{th} are as follows:

1 For $i = 2 : N-1,\ j = i+1 : N$, determine $Z_{ij}^{+},\ Z_{ij}^{-}$ from (15), (16). And the absolute difference between them as follows:

$$\epsilon_{ij} = abs\left(Z_{ij}^{+} - Z_{ij}^{-}\right) \tag{17}$$

2 For $i = 2 : N$, determine

$$S_i = \sum_{\substack{j=2 \\ j\ne i}}^{N}\epsilon_{ij} \tag{18}$$

3 Identify the DFT coefficient, k, with S_k the minimum of all S_i values, and take Z_k as the best possible estimate for Z_{th}.
4 Estimate E_{th} as follows:

$$E_{th} = \frac{\mathbf{V}_k + Z_{th}\mathbf{I}_k}{N} \tag{19}$$

2.3. The algorithm

The proposed method uses the DFT for determining the TE parameters of the system. As explained above, the proposed method recognizes and differentiates between three different situations. These are shown in Fig. 2. The steps of calculations are explained in the text and are shown by the flowchart of Fig. 3. As can be seen on the flowchart, the algorithm for determining TE parameters can be summarized as follows:

1 Get a new data window, N pairs of ($V,\ I$) measurements.
2 Determine the DFT coefficients for both current and voltage measurements $\mathbf{V}_k,\ \mathbf{I}_k,\ k$ using (5), (6).
3 Determine Z_k using (10) and compare the values of Z_k for $k = 2 :\ N$. If all Z_k are equal, then $Z_{th} = Z_k$, and determine E_{th} from (11): Go to step 1 to start a new calculation cycle, otherwise, else go to step 4.

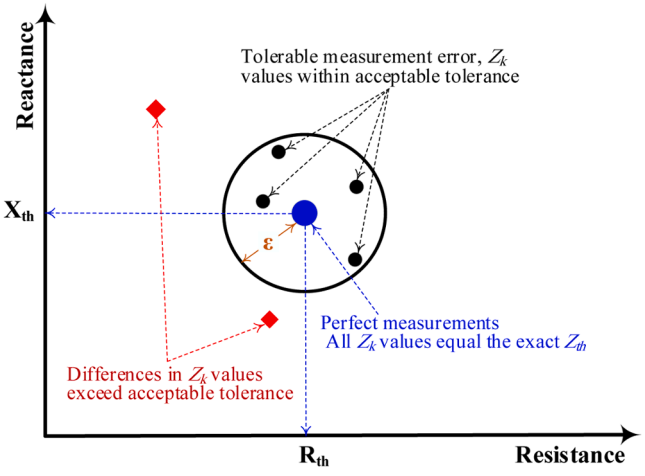

Fig. 2. Different cases of Z_{th} evaluation using DFT.

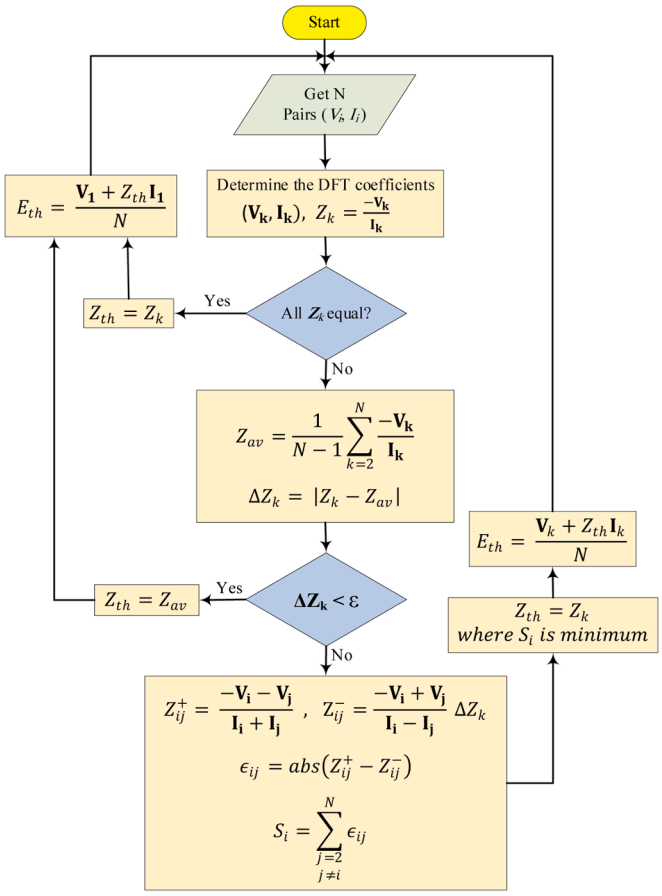

Fig. 3. Flow chart of the proposed method for TE parameter estimation.

4 Determine Z_{av} using (12), and ΔZ_k using (13); If all $\Delta Z_k \leq \varepsilon$, take $Z_{th} = Z_{av}$, and determine E_{th} from (11): Go to step 1 to start a new calculation cycle, otherwise go to step 5.
5 Do the steps defined by (15)–(17) and pick the k^{th} coefficient with the calculation of minimum of the differences let $Z_{th} = Z_k$, determine E_{th} from (19): Go to step 1 to start a new calculation cycle.

2.4. Identifying erroneous measurements

As explained in the previous section, in case of erroneous data, the best possible estimate for the TE parameters is obtained by the DFT coefficient with a minimum sum of differences between Z_{ij}^{+} and Z_{ij}^{-}. However, the accuracy of the TE estimate can be improved by identifying and excluding the bad measurement. The process of identifying the erroneous data uses the estimated TE along with the measured voltage/current phasors to calculate the corresponding current/voltage phasors. The calculated current/voltage phasors are compared to the measured values. The current/voltage measurement with the maximum deviation from the calculated one is identified as the erroneous one. TE is recalculated with identified erroneous measurement excluded. This process can be repeated until the Z_k values for all DFT coefficients are equal or within an acceptable tolerance.

3. Numerical applications

3.1. Illustrative example

The simple system of Fig. 4 is used to illustrate the determination of TE parameters using the DFT. The system has an ideal voltage source of 220 V connected to a load through a line with the impedance marked on the figure. The voltage at the load bus is determined at five different

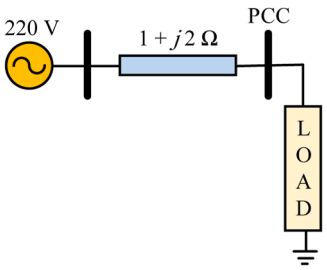

Fig. 4. A simple two bus system for illustrating the use of DFT to determine Thevenin equivalent parameters.

values of load currents; the voltage/current pairs are listed in Table 2. The DFT coefficients $\mathbf{V}_k$ and $\mathbf{I}_k$ are calculated using (5) and (6) respectively and listed in the first and second columns of Table 3. Impedance values calculated using (10) for $2 \leq k \leq 5$ are listed in the third column and the k[th] row of Table 3. The calculated E_{th} calculated by (11) is also listed in the first row and third column of Table 3. It is clear that DFT coefficients have perfectly determined the Thévenin equivalent parameters. This is of course because the data is error-free.

Now introducing an error in one of the measurements; –3% in I_5, the DFT is recalculated and the DFT coefficients are listed in Table 4. It can be noticed from the table that the Z_{th} estimated from the different DFT coefficients are not equal. Hence, E_{th} will assume a different value for each of Z_{th} values. This is why question marks are put against E_{th} in the table. The average value of Z_k, Z_{av}, is determined to be $1.091 + j1.936\ \Omega$. The deviations of Z_k values from the average, in per unit of the magnitude of Z_{av}, are listed in the last column in Table 4. Assuming a tolerable deviation of 5% in the magnitude of Z_{th}, all the Z_k values are within the acceptable tolerance and Z_{th} can be taken equal to Z_{av}, i.e. $Z_{th} = 1.091 + j1.936\ \Omega$, which is quite a good approximation to the actual value of $1 + j2\ \Omega$ with an error of less than 4%. E_{th} can be estimated using (11) to be $220.545 - j0.696\ V$, which is almost equal to the actual value of 220 V with an error of less than 0.3%.

It may be argued that each of the DFT coefficients is itself a kind of average and may not be wise to average what is already an average. However, in our case, the average and variance of Z_k values estimated from DFT are used just as indicators for the closeness of these values to each other and their usability for representing the system equivalent. The work of this paper recognizes the fact that DFT coefficients are weighted averages of the measurements. Of course, errors in measurements affect these averages. Error in one measurement sample affects the different DFT coefficients at different degrees. Hence, there will be the least affected DFT with the lowest effect due to error in the measurement. Therefore, in case of large variance of the estimated values of Z_k, the proposed method identifies the least affected DFT coefficient. This is used to determine the best estimate of Z_{th} out of the Z_k values as described by (15)–(18) and illustrated in the flowchart of Fig. 3.

For the purpose of illustration, the proposed method has been applied to the case of Table 2 above. Values of Z_k determined by (10) are listed on the main diagonal of Table 5. The values of Z_{ij}^{+}, as determined by (15) on the lower off-diagonal elements, and Z_{ij}^{-} as determined by (16) on the upper off-diagonal elements. The absolute differences, ϵ_{ij}, between Z_{ij}^{-} and Z_{ij}^{+}, for the DFT coefficient pairs are calculated using

Table 2
Voltage/Current pairs at the PCC of Fig. 4.

Voltage Phasor (V)	Current Phasor (I)
222.0 - j11.0	4.0 + j3.0
210.0 - j5.0	4.0 - j3.0
198.0 - j4.0	6.0 - j8.0
198.0 - j19.0	12.0 - j5.0
224.0 - j22.0	8.0 + j6.0

Table 3
DFT coefficients of voltage and current and the estimated E_{th} using (11), Z_{th} using (10).

$\mathbf{V_k}$ (V)	$\mathbf{I_k}$ (A)	Z_{th} (Ω)
1052 - j61.0	34.0 - j7.0	E_{th}= 220 V
60.727+ j12.579	−17.177 + j21.775	1.0 + j2.0
−11.016 + j11.965	−2.583 - j6.799	1.0 + j2.0
−2.469 – j 4.493	2.291 - j0.089	1.0 + j2.0
10.758 -j 14.051	3.469 + j7.113	1.0 + j2.0

Table 4
DFT coefficients of voltage and current and the estimated Z_{th} for erroneous data.

V_k (V)	I_k (A)	Z_k(Ω)	ΔZ_k (pu of Z_{av})
1052 - j61.0	33.760 - j7.18	E_{th}= ??	–
60.727+ j12.579	−17.08 + j21.49	1.018 + j2.017	0.0167
−11.016 + j11.965	−2.282 - j6.79	1.093 + j1.988	0.0211
−2.469 – j 4.493	2.379 + *j* 0.198	1.186 + j1.789	0.0337
10.758 -j 14.051	3.223+ j7.286	1.066 + j1.948	0.0004

Table 5
Z_{ij}^{+}(15), Z_{ij}^{-}(16) and Z_k (10).

		DFT Coefficient			
		2	3	4	5
DFT Coefficient	2	1.017+ j2.016	1.024+ j2.000	1.041+ j2.016	1.036+ j2.036
	3	1.018+ j2.040	1.092+ j1.988	1.065+ j1.932	1.078+ j1.967
	4	0.992+ j2.013	1.162+ j2.027	1.186+ j1.789	1.110+ j1.998
	5	1.012+ j1.997	1.126+ j1.630	1.056+ j1.898	1.066+ j1.948

(17) and listed in Table 6. The column sum of ϵ_{ij}, which is equal to S_i defined by (18), is calculated and listed in Table 6 at the bottom row. Knowing the TE parameters of the test system, which of course is not the case of a real system, some useful observations can be made out of Tables 5 and 6, which support the validity of the proposed method.

It can be noticed that the impedance values determined from individual DFT coefficients are not the same, which indicates the presence of measurement errors. It can also be noticed that some of the estimated impedance values are closer to the correct value than the others. In this example, the impedance estimated by the 2nd DFT coefficient is the nearest to the correct value. It has to be mentioned that this is not generic or even specific for this example system. It depends on the relative values of the samples and the order of the erroneous measurement sample. The general thing is that some calculated values will be less affected by the erroneous measurement than the others, which is clear in Table 5.

In Table 6, it is clear that the minimum sum of ϵ_{ij} is at the 2nd DFT coefficient indicating that Z_2 is the nearest to the correct Z_{th}. This proofs that the sum of ϵ_{ij} as proposed in this paper is a good indicator to the best estimate for Z_{th} should there be any erroneous measurements. The estimated TE parameters are thus $Z_{th} = 1.017 + j2.016\ \Omega$ and $E_{th} = 220.167 - j0.043\ V$.

Table 6
Values of ϵ_{ij} (17) for DFT coefficients.

		DFT Coefficient			
		2	3	4	5
DFT Coefficient	2	0.0	0.0408	0.0491	0.0465
	3	0.0408	0.0	0.1355	0.3412
	4	0.0491	0.1355	0.0	0.1133
	5	0.0465	0.3412	0.1133	0.0
	$S_i = \sum_{\substack{j=2 \\ j\neq i}}^{N} \epsilon_{ij}$	0.1364	0.5175	0.2979	0.5010

Although the estimated TE parameters seem to be close enough to the actual values, it can be further enhanced by identifying and excluding the erroneous measurement. The estimated TE parameters have been used to reproduce the voltage phasors corresponding to the measured current phasors. The estimated voltages and the differences between the measured and the estimated voltages, ΔV_i, are listed in Table 7. The same is done for the current phasors and the results are also listed in Table 7. It can be noticed that the largest differences ΔV_i and ΔV_i are those for the 5th sample. This means that the 5th sample is the erroneous one, which is exactly the case. Excluding this sample and recalculating the DFT for the remaining samples gives the exact value of TE parameters.

3.2. Test case (The IEEE 30 bus test system)

The IEEE 30 Bus test system is used as a test system, where the load at bus 30 is varied while keeping the rest of the system unchanged. The load at bus 30 is increased in small steps until the power flow diverged indicating the maximum loading condition. Voltage and current phasors at bus 30 are recorded and used with the proposed method to determine the TE parameters. A large number of cases were generated; the cases listed in Table 8 are just examples and may help whoever wants to work out the calculations. In the first test case, the calculated voltage and current phasors are kept ordered according to the increasing loading parameter at bus 30. Fig. 5 depicts the estimated TE parameters along with the load increase from its value at the standard base case up to the maximum loading,

It is to be mentioned that 5 Vage/current phasor pairs are used at each calculation cycle. The impedance values estimated from the different DFT coefficients are all shown in Fig. 5. It can be noticed the TE parameters calculated from all the different DFT coefficients are almost equal. Values of E_{th}, R_{th} and X_{th} at the base case loading are 1.048, 0.257, and 0.67 pu, which agree with the values reported for the same system in previous studies using different methods [2]. It can also be noticed that value of X_{th} slightly increases as the load increases. This is due to the increasing reactive power consumption near the maximum loading as the system gets nearer to the nose point of the Q/V curve.

To test the proposed method at conditions similar to online conditions of a real system, the data set generated for bus 30 of the IEEE test system was randomly reshuffled. A random error of normal distribution and zero average and standard deviation of 3% has been introduced to 20% of the current phasors. Five measurements are used in each calculation cycle, as recommended in [27]. This is why 20% of data are made erroneous; to guarantee that out of each 5 data points, one will have an error. The proposed method has been applied to modified data set and the results of the application are displayed in Fig. 6. In this figure, the TE equivalent parameters are estimated for the randomly shuffled data set before imposing the random error; this is termed as "Original". The TE for the data with the random errors before are indicated as "Erroneous" in the three parts of Fig. 6. The TE determined with identifying and excluding the erroneous data are termed as "Corrected". The upper part of Fig. 6 presents E_{th}; the middle part presents X_{th} and the lower part displays R_{th} for the three mentioned conditions. It is clear from the figure that the proposed method was able to track the TE parameters despite the random variations of the load. It is also clear that

Table 7
Estimated Voltage and Current Samples and The Error.

Sample No.	V_i	ΔV_i	I_i	ΔI_i
1	222.15 - j11.16	0.220	3.965 + j2.91	0.098
2	210.05-j 5.06	0.074	3.986- j3.03	0.033
3	197.93 -j4.00	0.074	5.984 - j7.97	0.033
4	197.87 - j19.16	0.204	11.912 - j4.98	0.090
5	224.01 - j21.62	0.383	7.913 + *j* 5.89	0.170

Table 8
Voltage and Current Phasors For Different Loading Conditions at Bus 30 of The IEEE 30 Bus System.

	∠V	|I|	∠ I
1.0395	−9.76	0.0207	−19.92
1.0231	−11.17	0.0632	−21.33
1.0056	−12.63	0.1071	−22.79
0.9962	−13.39	0.1297	−23.55
0.9657	−15.77	0.2007	−25.93
0.9546	−16.61	0.2256	−26.77
0.9429	−17.47	0.2513	−27.63
0.9035	−20.27	0.3337	−30.43
0.7242	−31.61	0.6542	−41.77
0.6327	−36.81	0.7919	−46.97

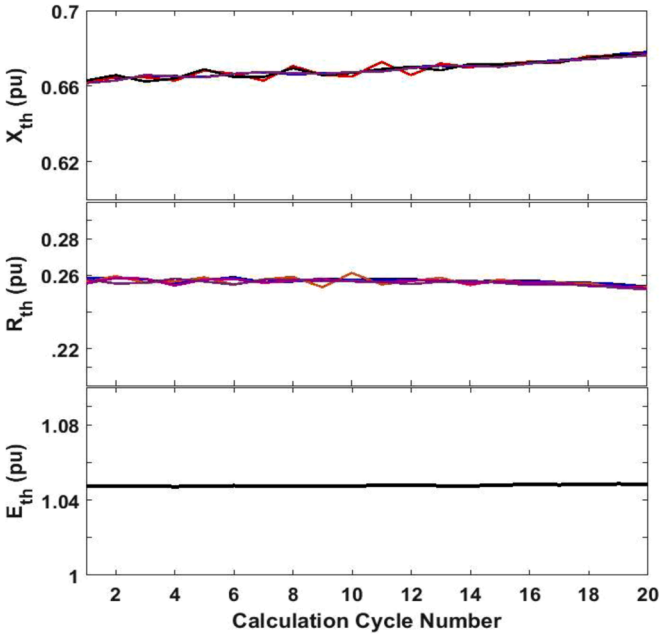

Fig. 5. TE parameters of the IEEE 30 bus test system at bus 30 for gradual load increase.

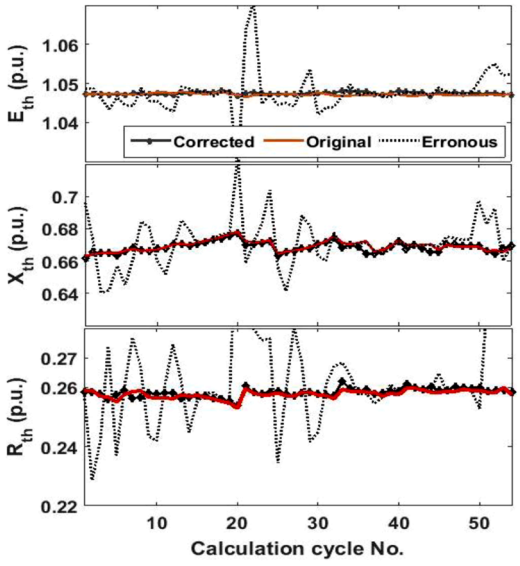

Fig. 6. TE parameters of the IEEE 30 bus test system at bus 30 for random load variations and measurement errors.

the proposed method has been able to deal with errors in the TE parameters values caused by errors in measurements. The figure makes it clear that estimated TE parameters by the introduced procedure for detecting erroneous data in an almost perfect agreement with those determined using the error-free original data.

It is worth mentioning that the maximum per unit error in the estimated TE parameters is found to be about three times the standard deviation of the error intentionally imposed onto the data points used. This illuminates on the need of high accuracy measurements and the regular calibration of the PMUs and any other measuring devices used.

4. Conclusion

This paper presented a new method for online tracking of Thevenin equivalent parameters at a node in a power system. The method builds on DFT and is utilized to determine the TE parameters, test the accuracy of the estimated TE, and check for the existence of bad data. Also, a simple yet effective procedure for identifying and excluding bad data is presented. The method is illustrated in detail using a simple two-node system and is tested using the IEEE 30 bus test system.

Results of application to the IEEE 30 bus test system proved the effectiveness of the method in determining a reliable TE for a power system even in the presence of erroneous measurements. The method is simple and can be used for online applications and can be simply implemented within the PMU as an additional function to deliver the TE at the measurement location. It can also be used for education purposes.

CRediT authorship contribution statement

Abdelrahman Sobhy: Conceptualization, Methodology, Data curation, Writing – original draft. **Mohammed A. Saeed:** Conceptualization, Methodology, Investigation, Software. **Abdelfattah A. Eladl:** Conceptualization, Methodology, Resources, Validation. **Sobhy M. Abdelkader:** Conceptualization, Methodology, Supervision, Writing – review & editing.

Declaration of Competing Interest

The authors declare that they have no known competing financial interests or personal relationships that could have appeared to influence the work reported in this paper.

References

[1] A.H. Al-Mohammed, M.A. Abido, A fully adaptive PMU-based fault location algorithm for series-compensated lines, IEEE Trans. Power Syst. 29 (5) (2014), https://doi.org/10.1109/TPWRS.2014.2303207.
[2] M.M. El-Kateb, S. Abdelkader, M.S. Kandil, Linear indicator for voltage collapse in power systems, IEE Proc. Gener. Transm. Distrib. 144 (2) (1997), https://doi.org/10.1049/ip-gtd:19970801.
[3] B.C. Karatas, H. Jóhannsson, A.H. Nielsen, Voltage stability assessment accounting for non-linearity of Thévenin voltages, IET Gener. Transm. Distrib. 14 (16) (2020), https://doi.org/10.1049/iet-gtd.2019.1774.
[4] H.Y. Su, T.Y. Liu, Robust thevenin equivalent parameter estimation for voltage stability assessment, IEEE Trans. Power Syst. 33 (4) (2018), https://doi.org/10.1109/TPWRS.2018.2821926.
[5] J. Lavenius, L. Vanfretti, and G. N. Taranto, "Performance assessment of PMU-based estimation Methods of Thevenin Equivalents for real-time voltage stability monitoring," IEEE 15th International Conference on Environment and Electrical Engineering (EEEIC), Rome, Italy, 10-13 June 2015., doi: 10.1109/EEEIC.2015.7165477.
[6] Y. Wang, W. Li, J. Lu, A new node voltage stability index based on local voltage phasors, Electr. Power Syst. Res. 79 (1) (2009), https://doi.org/10.1016/j.epsr.2008.06.010.
[7] Y. Wang, et al., Voltage stability monitoring based on the concept of coupled single-port circuit, IEEE Trans. Power Syst. 26 (4) (2011), https://doi.org/10.1109/TPWRS.2011.2154366.
[8] S. Shen, et al., An adaptive protection scheme for distribution systems with dgs based on optimized thevenin equivalent parameters estimation, IEEE Trans. Power Deliv. 32 (1) (2017), https://doi.org/10.1109/TPWRD.2015.2506155.

[9] S.M. Mazhari, N. Safari, C.Y. Chung, I. Kamwa, A hybrid fault cluster and thévenin equivalent based framework for rotor angle stability prediction, IEEE Trans. Power Syst. 33 (5) (2018), https://doi.org/10.1109/TPWRS.2018.2823690.
[10] B.K. Karmakar, A.K. Pradhan, Detection and classification of faults in solar PV array using thevenin equivalent resistance, IEEE J. Photovoltaics 10 (2) (2020), https://doi.org/10.1109/JPHOTOV.2019.2959951.
[11] L. Peng, J. Zhao, Y. Tang, L. Mili, Z. Gu, Z. Zheng, Real-time LCC-HVDC maximum emergency power capacity estimation based on local PMUs, IEEE Trans. Power Syst. 36 (2) (2021), https://doi.org/10.1109/TPWRS.2020.3021099.
[12] M. Ghafouri, M. Au, M. Kassouf, M. Debbabi, C. Assi, J. Yan, Detection and mitigation of cyber attacks on voltage stability monitoring of smart grids, IEEE Trans. Smart Grid 11 (6) (2020), https://doi.org/10.1109/TSG.2020.3004303.
[13] S.A. Arefifar, W. Xu, Online tracking of power system impedance parameters and field experiences, IEEE Trans. Power Deliv. 24 (4) (2009), https://doi.org/10.1109/TPWRD.2009.2021046.
[14] S.J.S. Tsai, K.H. Wong, On-line estimation of Thevenin equivalent with varying system states,", in: IEEE Power and Energy Society General Meeting-Conversion and Delivery of Electrical Energy in the 21st Century, Pittsburgh, USA, 2008, https://doi.org/10.1109/PES.2008.4596364, 20-24 July.
[15] Y. Liu, Z. Li, Y. Yang, J. Liu, A novel on-line identification for Thevenin equivalent parameters of power system regarding persistent disturbance condition,", in: China International Conference on Electricity Distribution, CICED, 2016, https://doi.org/10.1109/CICED.2016.7575909 vol. 2016-September.
[16] M. Esparza, J. Segundo, C. Gurrola-Corral, N. Visairo-Cruz, E. Barcenas, E. Barocio, Parameter estimation of a grid-connected VSC using the extended harmonic domain, IEEE Trans. Ind. Electron. 66 (8) (2019), https://doi.org/10.1109/TIE.2018.2870404.
[17] L. Asiminoaei, R. Teodorescu, F. Blaabjerg, U. Borup, Implementation and test of an online embedded grid impedance estimation technique for PV inverters, IEEE Trans. Ind. Electron. 52 (4) (2005), https://doi.org/10.1109/TIE.2005.851604.
[18] N. Hoffmann, F.W. Fuchs, Minimal invasive equivalent grid impedance estimation in inductive-resistive power networks using extended Kalman filter, IEEE Trans. Power Electron. 29 (2) (2014), https://doi.org/10.1109/TPEL.2013.2259507.
[19] B.L. Eidson, D.L. Geiger, M. Halpin, Equivalent power system impedance estimation using voltage and current measurements,", in: IEEE Clemson University Power Systems Conference, Clemson, SC, USA, 2014, https://doi.org/10.1109/PSC.2014.6808107, 11-14 March.
[20] Y. Wang, W. Xu, J. Yong, An adaptive threshold for robust system impedance estimation, IEEE Trans. Power Syst. 34 (5) (2019), https://doi.org/10.1109/TPWRS.2019.2924349.
[21] A. Malkhandi, N. Senroy, S. Mishra, A dynamic model of impedance for online thevenin's equivalent estimation, IEEE Trans. Circuits Syst. II Express Briefs 7747 (c) (2021) 1–5, https://doi.org/10.1109/TCSII.2021.3085186.
[22] A. Arancibia, C.A. Soriano-Rangel, F. Mancilla-David, R. Ortega, K. Strunz, Finite–time identification of the Thévenin equivalent parameters in power grids, Int. J. Electr. Power Energy Syst. 116 (2020), https://doi.org/10.1016/j.ijepes.2019.105534.
[23] Z. Yun, X. Cui, K. Ma, Online thevenin equivalent parameter identification method of large power grids using LU factorization, IEEE Trans. Power Syst. 34 (6) (2019), https://doi.org/10.1109/TPWRS.2019.2920994.
[24] K. Vu, Use of local measurements to estimate voltage-stability margin, IEEE Trans. Power Syst. 14 (3) (1999), https://doi.org/10.1109/59.780916.
[25] M.M. Haji, W. Xu, Online determination of external network models using synchronized phasor data, IEEE Trans. Smart Grid 9 (2) (2018), https://doi.org/10.1109/TSG.2016.2559486.
[26] S. Corsi, G.N. Taranto, A real-time voltage instability identification algorithm based on local phasor measurements, IEEE Trans. Power Syst. 23 (3) (2008), https://doi.org/10.1109/TPWRS.2008.922586.
[27] S.M. Abdelkader, D.J. Morrow, Online tracking of thévenin equivalent parameters using PMU measurements, IEEE Trans. Power Syst. 27 (2) (2012), https://doi.org/10.1109/TPWRS.2011.2178868.
[28] B. Alinezhad, H.K. Karegar, On-line thévenin impedance estimation based on PMU data and phase drift correction, IEEE Trans. Smart Grid 9 (2) (2018), https://doi.org/10.1109/TSG.2016.2574765.
[29] I. Šmon, G. Verbič, F. Gubina, Local voltage-stability index using Tellegen's theorem, IEEE Trans. Power Syst. 21 (3) (2006), https://doi.org/10.1109/TPWRS.2006.876702.
[30] A.R. Ramapuram Matavalam, V. Ajjarapu, Sensitivity based thevenin index with systematic inclusion of reactive power limits, IEEE Trans. Power Syst. 33 (1) (2017), https://doi.org/10.1109/tpwrs.2017.2701811.
[31] S.M. Abdelkader, D.J. Morrow, Online thévenin equivalent determination considering system side changes and measurement errors, IEEE Trans. Power Syst. 30 (5) (2015), https://doi.org/10.1109/TPWRS.2014.2365114.
[32] S.M. Burchett, et al., An optimal thévenin equivalent estimation method and its application to the voltage stability analysis of a wind hub, IEEE Trans. Power Syst. 33 (4) (2018), https://doi.org/10.1109/TPWRS.2017.2776741.
[33] S.M. Abdelkader, A.A. Eladl, M.A. Saeed, D.J. Morrow, Online thévenin equivalent determination using graphical phasor manipulation, Int. J. Electr. Power Energy Syst. 97 (2018), https://doi.org/10.1016/j.ijepes.2017.11.013.
[34] M.N. Islam, W. Ongsakul, Thevenin Equivalent Parameter Tracking For On-Line Voltage Stability Assessment, 3-6, IEEE Innovative Smart Grid Technologies-Asia (ISGT ASIA), Bangkok, Thailand, Nov. 2015, https://doi.org/10.1109/ISGT-Asia.2015.7387027.
[35] C. Wang, Z. Qin, Y. Hou, J. Yan, Multi-area dynamic state estimation with PMU measurements by an equality constrained extended kalman filter, IEEE Trans. Smart Grid 9 (2) (2018), https://doi.org/10.1109/TSG.2016.2570943.
[36] N. Zhou, D.J. Trudnowski, J.W. Pierre, W.A. Mittelstadt, Electromechanical mode online estimation using regularized robust RLS methods, IEEE Trans. Power Syst. 23 (4) (2008), https://doi.org/10.1109/TPWRS.2008.2002173.
[37] E. Peker, A. Wiesel, Fitting generalized multivariate huber loss functions, IEEE Signal Process. Lett. 23 (11) (2016), https://doi.org/10.1109/LSP.2016.2612170.
[38] T. An, S. Zhou, J. Yu, W. Lu, Y. Zhang, Research On Illed-Conditioned Equations in Tracking Thevenin Equivalent Parameters With Local Measurements, 22-26, IEEE International Conference on Power System Technology, Chongqing, China, Oct. 2006, https://doi.org/10.1109/ICPST.2006.321574.
[39] I.L. Roca, P.M.S. Carvalho, Solving Ill-conditioned state-estimation problems in distribution grids with hidden-markov models of load dynamics, IEEE Trans. Power Syst. 35 (1) (2020), https://doi.org/10.1109/TPWRS.2019.2928211.
[40] N. Zhou, J.W. Pierre, D.J. Trudnowski, R.T. Guttromson, Robust RLS methods for online estimation of power system electromechanical modes, IEEE Trans. Power Syst. 22 (3) (2007), https://doi.org/10.1109/TPWRS.2007.901104.
[41] N. Mohammed, M. Ciobotaru, G. Town, Online parametric estimation of grid impedance under unbalanced grid conditions, Energies 12 (24) (2019), https://doi.org/10.3390/en12244752.
[42] J.H. Suárez, H.M.T.C. Gomes, A.J. Sguarezi Filho, D.A. Fernandes, F.F. Costa, Grid impedance estimation for grid-tie inverters based on positive sequence estimator and morphological filter, Electr. Eng. 102 (3) (2020), https://doi.org/10.1007/s00202-020-00941-8.